

## Red photonic glasses and confined structures

R.R. GONÇALVES<sup>1</sup>, A. LUKOWIAK<sup>2</sup>, D. RISTIC<sup>3</sup>, B. BOULARD<sup>4</sup>, A. CHIAPPINI<sup>5</sup>,  
A. CHIASERA<sup>5</sup>, D. DOROSZ<sup>6</sup>, M. MARCINIAK<sup>7</sup>, G.C. RIGHINI<sup>8,9</sup>, and M. FERRARI<sup>5,8\*</sup>

<sup>1</sup> Departamento de Química, Faculdade de Filosofia, Ciências e Letras de Ribeirão Preto, Universidade de São Paulo – Av. Bandeirantes, 3900, CEP 14040-901, Ribeirão Preto/SP, Brazil

<sup>2</sup> Institute of Low Temperature and Structure Research, PAS, 2 Okolna St., 50-422 Wrocław, Poland

<sup>3</sup> Ruder Bošković Institute, P.O. Box 180, 10002 Zagreb, Croatia

<sup>4</sup> Institut des Molécules et Matériaux du Mans, UMR 6283, Equipe Fluorures, Université du Maine, Av. Olivier Messiaen, 72085 Le Mans cedex 09, France

<sup>5</sup> IFN – CNR CSMFO Lab., Via alla Cascata 56/C Povo, 38123 Trento, Italy

<sup>6</sup> Department of Power Engineering, Photonics and Lighting Technology, Bialystok University of Technology, 45D Wiejska St., Białystok, 15-351, Poland

<sup>7</sup> National Institute of Telecommunications, 1 Szachowa St., 04 894 Warsaw, Poland

<sup>8</sup> Museo Storico della Fisica e Centro di Studi e Ricerche Enrico Fermi, Piazza Viminale 1, 00184 Roma, Italy

<sup>9</sup> IFAC – CNR, MiPLab, Via Madonna del Piano 10, 50019 Sesto Fiorentino, Italy

**Abstract.** We present some recent results obtained by our team in rare earth doped photonic glasses and confined structures, in order to give some highlights regarding the state of art in glass photonics. To evidence the unique properties of transparent glass ceramics we compare spectroscopic and structural properties between the parent glass and the glass ceramics. Starting from planar waveguides we move to spherical microresonators, a very interesting class of photonic confined structures. We also conclude the short review with some remarks about the perspective for glass photonics.

**Key words:** glass photonics, rare earth ions, waveguides, integrated optics, glass ceramics, microspheres, whispering gallery modes, SiO<sub>2</sub>-HfO<sub>2</sub>; SiO<sub>2</sub>-SnO<sub>2</sub>.

### 1. Introduction

Glass photonics is pervasive in a huge number of human activities and drives the research in the field of enabling technologies [1–3]. The fruitful exploitation of glass photonics is not restricted only to the area of Information and Communication Technology. Many other photonic devices, with a large spectrum of applications covering Health and Biology, Structural Engineering, and Environment Monitoring Systems, have been developed during the last years. Glass materials and photonic structures are the cornerstones of scientific and technological building in integrated optics. Photonic glasses, optical glass waveguides, planar light integrated circuits, waveguide gratings and arrays, functionalized waveguides, photonic crystal heterostructures, and hybrid microresonators are some examples of glass-based integrated optical devices that play a significant role in optical communication, sensing, biophotonics, processing, and computing. This cross-disciplinary approach leads to constructed luminescent structures that can perform sensing and functionalized structures to successfully address socioeconomic challenges, such as security, cost-effective healthcare, energy savings, efficient and clean industrial production, environmental protection, and fast and efficient communications. Photonics, with its pervasiveness, has already been identified as an enabling

technology, and through advanced research in glass-based integrated optics systems, photonics can contribute to finding new technical solutions to still unsolved problems, and pave the way to applications not yet imagined [3].

Even if several glass-based devices are actually available on the market, at the state of the art the strength of the research on novel glasses is focused on optimizing chemical composition and developing innovative fabrication processes, in order to reduce the costs and increase the performances of the devices so obtained. The research becomes more and more attractive when luminescent ions are incorporated in the glass. The well-known tutorial example is the successful application in telecommunication of Wavelength Division Multiplexing (WDM) components and Erbium-Doped Fiber Amplifiers (EDFAs). Although silicate glasses still maintain a consolidated place as materials for photonic, the soft glasses are largely investigated because they offer a much broader transmission window in the infrared, higher refractive index, and a much higher nonlinear refractive index. As a consequence, interesting confined structures obtained by tellurite, fluoride, and chalcogenide glasses, as well as by polymers, have been demonstrated [4–7].

Rare-earth-doped (RED) photonic glasses and photonic structures, so called RED glass, is the topic of the present paper. We give a short overview of some interesting struc-

\*e-mail: maurizio.ferrari@ifn.cnr.it

tures at nano- and microscale, where the luminescence of the rare earth ions can be tailored or enhanced playing with the energy transfer mechanism and controlling the average spatial distribution of the lanthanides. Very briefly we will remind rare-earth-activated amorphous waveguide structures that represent the consolidated cornerstone in a wide number of technological applications such as integrated optical amplifiers, laser systems, and very recently solar energy converters [8–10]. Then we introduce some significant aspects of glass ceramics and we close the paper mentioning some highlights about microresonators and microcavities.

## 2. Rare earth-doped planar waveguides

$\text{Er}^{3+}$  doped silicate waveguides have been the subject of extensive research as optical confined structures for photonics application, due to the coincidence of the  $\text{Er}^{3+}$  emission band around  $1.5 \mu\text{m}$  with the lowest loss window of silica-based fiber optic telecommunications systems. The small absorption cross section of Erbium compared to other optical active species [11] is one of the principal troubles connected to the optimization of the excitation efficiency of erbium activated glasses for photonics application. A number of solutions has been studied in order to permit the increase of the total absorption cross section of the whole system, with the aim to enhance the spectroscopic properties of erbium ions at  $1.5 \mu\text{m}$ . Under this perspective several kinds of rare earth sensitizers including semiconductor nanocrystals [12–14] and metallic nanoparticles [15] have been investigated.

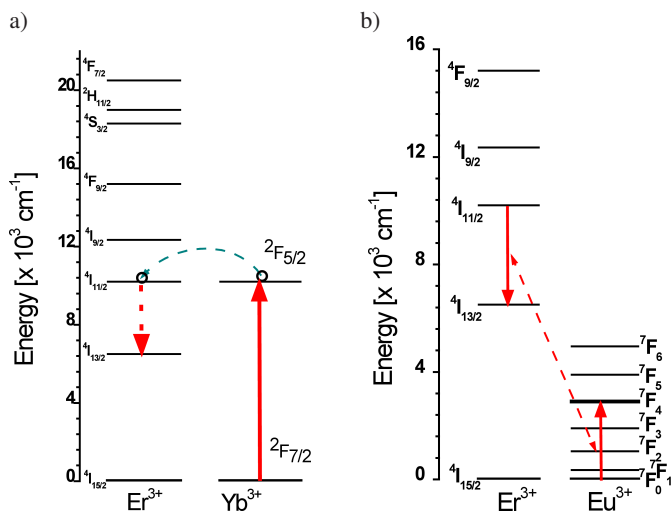


Fig. 1. a)  $\text{Yb}^{3+}$  ion as  $\text{Er}^{3+}$  ion sensitizer. This is the standard approach used for  $\text{Er}^{3+}$  pumping; b) cross relaxation mechanism  $\text{Er}^{3+}/\text{Eu}^{3+}$  employed to increase the  ${}^4\text{I}_{13/2}$  level population

A lot of research groups have focused their attention in the preparation of erbium doped glasses codoped with different kind of rare earth ions. It has been shown, that the introduction of ytterbium ions enhances the system absorption at 980 nm, making the pumping mechanism more efficient [11, 16–18]. Furthermore, the introduction of rare earths such as  $\text{Eu}^{3+}$ ,  $\text{Ce}^{3+}$ , or  $\text{Tb}^{3+}$ , has been studied in order to increase

the transition rate between the  ${}^4\text{I}_{11/2}$  and the  ${}^4\text{I}_{13/2}$  levels [7, 19]. Until now, the effect of the introduction of  $\text{Eu}^{3+}$  and  $\text{Ce}^{3+}$ , has been studied in system with a very low phonon energy and therefore, with small non-radiative transition rate. Anyway, in principle the just described effect could be observable also in multicomponent glasses, having in mind a preferential position of the rare earth ions closer to the component with the lower phonon energy, as hafnia could be the case [19]. Figure 1 shows the relevant  $\text{Er}^{3+}$ ,  $\text{Yb}^{3+}$  (Fig. 1a) and  $\text{Er}^{3+}$ ,  $\text{Eu}^{3+}$  (Fig. 1b) energy levels with the description of the two different processes that can enhance the spectroscopic characteristics of  $\text{Er}^{3+}$  at  $1.5 \mu\text{m}$ .

In fact, several studies have been developed on the basis of silica-hafnia and fluoride waveguiding systems [20–22]. The fabrication protocol of amorphous silica-hafnia waveguides by the sol-gel route is now well consolidated. Nevertheless, optimization of the composition, still remain the first requirement to obtain suitable waveguiding structures. Two aspects will be considered here: i) the role of hafnia concentration on the structural and optical properties; ii) the role of  $\text{Er}^{3+}$  content on the luminescence efficiency. As far as the role of hafnia concentration on the spectroscopic properties is concerned, we observed that the bandwidth of the  ${}^4\text{I}_{13/2} \rightarrow {}^4\text{I}_{15/2}$  emission is practically independent on the composition of the waveguide. This is due to the fact that  $\text{HfO}_2$  promotes a disruption of the silica network, as we proved by Raman measurements [9, 22, 23]. As a consequence,  $\text{Hf}^{4+}$  increases the number of Si-O non-bridging groups accounting for a general network flexibility, which may accommodate  $\text{Er}^{3+}$  contents without appreciable matrix strains. The  ${}^4\text{I}_{13/2}$  lifetime decreases with the increasing of the  $\text{HfO}_2$  molar concentration. This is an interesting point related to the role of hafnia. EXAFS measurements performed on the  $\text{SiO}_2\text{-HfO}_2$  waveguides have demonstrated that  $\text{Er}^{3+}$  ions are preferentially dispersed in  $\text{HfO}_2$ -rich regions of the glassy waveguide, even at the lowest  $\text{HfO}_2$  concentration [24]. The  ${}^4\text{I}_{13/2}$  lifetime shortening can be explained by considering that the incorporation of  $\text{HfO}_2$  in silica strongly modifies the next-nearest shell environment around  $\text{Er}^{3+}$  ion, inducing an increase of the electric dipole component of the  ${}^4\text{I}_{13/2} \rightarrow {}^4\text{I}_{15/2}$  transition probability. Higher is the hafnia content higher is the probability for  $\text{Er}^{3+}$  ion to find Hf in its second coordination shell, then enhancing the radiative relaxation rate. Spectroscopic and optical measurements have demonstrated that the most efficient compositions are 70:30 and 60:40 ( $\text{SiO}_2\text{:HfO}_2$ ). For both compositions we obtain very similar spectroscopic properties with a reasonable annealing time. However, the two compositions are not equivalent. In fact, X-ray photoelectron spectroscopy measurements performed on the amorphous waveguides as a function of hafnia content allowed us to identify both structural changes and the 40 mol% as critical  $\text{HfO}_2$  abundance at which the phase separation occurs [25]. On the basis of these results optimized RED silica-hafnia planar waveguides for integrated optics were obtained. The Figure of Merit is given in Table 1. A rib waveguide obtained by dry-etching process is reported in Fig. 2 as well as the integrated waveguide laser is reported in Fig. 3.

Table 1

Figure of Merit of optimized silica-hafnia planar waveguides for integrated optics

SiO <sub>2</sub> /HfO <sub>2</sub> molar ratio	Er <sup>3+</sup> [mol%]	Confinement coefficient @ 1542 nm	Propagating mode @ 1542 nm
70:30	0.3	0.81	1
Losses @ 1542 nm [± 0.3dB/cm]	Quantum efficiency	<sup>4</sup> I <sub>13/2</sub> lifetime ± 0.5 [ms]	<sup>4</sup> I <sub>13/2</sub> → <sup>4</sup> I <sub>15/2</sub> bandwidth ± 2 [nm]
< 0.3	88%	5.9	50

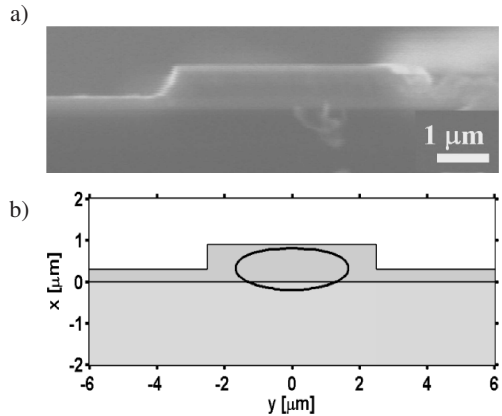


Fig. 2. a) SEM microphoto of a channel waveguide obtained by a dry-etching process on 70SiO<sub>2</sub>-30HfO<sub>2</sub> planar waveguide fabricated by sol-gel route; b) schematic cross section of the rib silica-hafnia waveguide showing the 2/3 mode intensity contour after Ref. 23

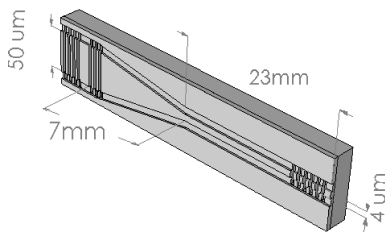


Fig. 3. Schematic view of the Nd<sup>3+</sup> doped silica-hafnia tapered rib waveguide laser obtained by sol-gel route. The external grating on the left is used as input for the pump and output for the pump, exploiting the dependence on the resonant coupling angles. The cavity is constituted by a partial reflecting grating on the left and a total reflecting grating on the right end facet after Ref. 8

### 3. Rare earth-doped transparent glass ceramics

Glass-ceramics are nanocomposite materials which offer specific characteristics of capital importance in photonics. This kind of two-phase materials is constituted by nanocrystals embedded in a glass matrix and the respective composition and volume fractions of crystalline and amorphous phase determine the properties of the glass-ceramic. Among these properties transparency is crucial, in particular when confined structures, such as dielectric optical waveguides, are considered and several works have been devoted to this topic. Another important point is the role of the nanocrystals when activated by luminescent species, as rare earth ions, and their effect on the spectroscopic properties of the glass-ceramic. The presence of the crystalline environment around the rare earth ion

allows high absorption and emission cross sections, reduction of the non-radiative relaxation thanks to the lower phonon cut-off energy, and tailoring of the ion-ion interaction by the control of the rare earth ion partition. Fabrication, assessment and application of glass-ceramic photonic systems, especially waveguides, deserve an appropriate discussion which is the aim of this section, focused on luminescent glass-ceramics.

A rare earth-activated glass-ceramic waveguide constitutes a potential significant system to behave as an effective optical medium for light propagation and luminescence enhancement. In 1998 Tick published a paper with the explicit title “Are low-loss glass-ceramic optical waveguides possible?” [26]. The answer was positive and he concluded the paper suggesting that the minimum transmission loss limit of the investigated effective medium glass ceramics is in the order of tens of decibels per kilometer, once all of the impurities can be eliminated. In the same paper some general criteria for light propagation are given. These criteria concern nanocrystals size, narrow particle-size distribution, inter-particle spacing, and clustering. As far as concerns scattering attenuation, it is important to note that the transparency of glass-ceramics is higher than that expected from the theory of Rayleigh scattering. Edgar et al. measured the optical extinction coefficient for fluorozirconate glass-ceramics containing BaCl<sub>2</sub> nanoparticles and found that glass-ceramics were about a factor of six more transparent than predicted by Rayleigh scattering theory [27]. Looking at the general criteria given above, the main reason of such behavior appears to be related to the spatial arrangement and the consequent interference pattern of the scattered light [26]. A further important step in the understanding and estimation of quenching of the Rayleigh scattering in glass-ceramic was given by Mattarelli et al. [15]. These authors put in evidence the important role played by the structure factor of the system and demonstrate that the physical mechanism producing high transparency in glass-ceramics is the low density fluctuation in the number of scatterers [15].

The important statement given by Tick sixteen years ago was that glass-ceramics will certainly be legitimate candidates for use in most photonic devices. Now, this expectation is a reality, as demonstrated by several glass-ceramic-based systems reported in literature where the common goal is the waveguiding property [28, 13]. From a general point of view it is evident that RED integrated optical amplifiers and laser systems exhibit chemical and physical effects, mainly linked to the ion-ion interactions as well as to the nonradiative relaxation processes, which are detrimental for the efficiency of active waveguide and have been the subject of several scientific and technological investigations [2]. Glass-ceramic waveguides can contribute to overcome some of the above mentioned problems. These composite materials allow the control of the chemical environment of the rare earth ion, and thus reduce the chemical clusters and the consequent luminescence quenching. Moreover, glass-ceramic waveguides are a valid alternative to the widely used glass hosts such as silica, which has a high phonon energy of 1100 cm<sup>-1</sup>. In fact, the embedded rare-earth-doped nanocrystals with low cutoff vibrational energy, such as hafnia, fluoride, titania, tin oxide,

and zirconia, reduce the nonradiative contribution to the relaxation mechanism, allowing high fluorescence efficiency. Finally, some kind of nanocrystals such as SnO<sub>2</sub> have demonstrated to be excellent rare earth sensitizers and excellent SiO<sub>2</sub>-SnO<sub>2</sub> waveguides have been demonstrated [12–14]. We want close this section about glass-ceramics pointing out the advantage of this system for energy transfer optimization.

Table 2

Estimated transfer efficiency and estimated effective quantum efficiency as a function of Yb<sup>3+</sup> molar concentration for a glass-ceramic silica-hafnia waveguide where Tb<sup>3+</sup> content is fixed at 0.5 mol%. The results obtained for the parent glass matrix are also reported

Composition (Yb concentration in mol%)	1%	2%	3%
Estimated transfer efficiency (in glass-ceramic)	14%	24%	25%
Estimated transfer efficiency (in parent glass)	2%	4%	6%

During the last years several work has been performed in order to develop energy transfer based systems for photoluminescence application. In this scientific area we have up- and down-converters planar waveguides for integrated optics [29], visible laser light sources and solar cells efficiency enhancement [21, 30, 31], specific nanostructured system used as sensitizers of rare earth luminescence [32].

Figure 4a–c shows the energy transfer mechanisms for the donor-acceptor Tb<sup>3+</sup>/Yb<sup>3+</sup>, Yb<sup>3+</sup>/Pr<sup>3+</sup>, and Pr<sup>3+</sup>/Yb<sup>3+</sup> couples, respectively. Figure 4a discusses a simple example where, starting from a visible photon, we can obtain two photons at 980 nm thanks to the Tb<sup>3+</sup> → Yb<sup>3+</sup> energy transfer. The host matrix is constituted by a waveguide of molar composition 70SiO<sub>2</sub>-30HfO<sub>2</sub>. The amorphous and glass ceramic waveguides were prepared by sol-gel route using the dip-coating technique and a specific annealing procedure as reported in [23, 29]. We demonstrated that glass ceramic increases the energy transfer efficiency compared to the parent glass as clearly shown in Table 2 [30]. This effect is a consequence of the reduction of non-radiative relaxation channels

due to the low cut off frequency of HfO<sub>2</sub> nanocrystals that plays a capital role in the energy transfer efficiency between Tb<sup>3+</sup> and Yb<sup>3+</sup> ions. Moreover, as mentioned above, the crystalline environment for the rare earth ions maintains a suitable distance among the ions reducing the concentration quenching due to physical clustering. Figures 4b and 4c show the energy level diagram demonstrating the possible energy transfers between Pr<sup>3+</sup> and Yb<sup>3+</sup> ions in (b) up-conversion and (c) down-conversion processes. Even in this case low phonon energy host is recommended and recently we presented a work regarding fluoride-based waveguide glass-ceramics [21, 31]. The up-conversion emission can be explained by an energy transfer from Yb<sup>3+</sup> to Pr<sup>3+</sup>. In a first step, a 980 nm pump photon provokes the excitation of Yb<sup>3+</sup> from <sup>2</sup>F<sub>7/2</sub> to <sup>2</sup>F<sub>5/2</sub> state. The excited Yb<sup>3+</sup> transfers its energy to a neighbor Pr<sup>3+</sup> ion in the <sup>3</sup>H<sub>4</sub> ground state, promoting it to the <sup>1</sup>G<sub>4</sub> excited state. The excited Pr<sup>3+</sup> ion absorbs a pump photon leading to a transition to the <sup>3</sup>P<sub>0</sub> upper level. Finally, the Pr<sup>3+</sup> ion decays from the <sup>3</sup>P<sub>0</sub> level or from the thermalized <sup>3</sup>P<sub>1</sub> level to generate the visible emissions (Fig. 4b). The up-conversion emission increases linearly with the ytterbium sensitizer concentration for glass ceramic, consistent with just one step energy transfer process. In the case of the glasses, the curve dependence of the upconverted intensity as a function of Yb<sup>3+</sup> content evidences a deviation from the linear behavior starting from 2 mol% Yb<sup>3+</sup> content. The energy transfer rate reduction is due to energy back transfer from Pr<sup>3+</sup> to Yb<sup>3+</sup> and to a decrease of the Yb<sup>3+</sup> lifetime caused by concentration quenching. The concentration quenching is strongly reduced in glass ceramic, as can be proved by the behavior of the <sup>3</sup>P<sub>0</sub> decay curves, thanks to modification of rare earth repartition in the glassy and crystal phases. While the emission intensity in glass seems to reach a plateau at low Yb<sup>3+</sup> content, around 3 mol%, the upconverted emission could increase beyond 5 mol% Yb<sup>3+</sup> in glass-ceramics.

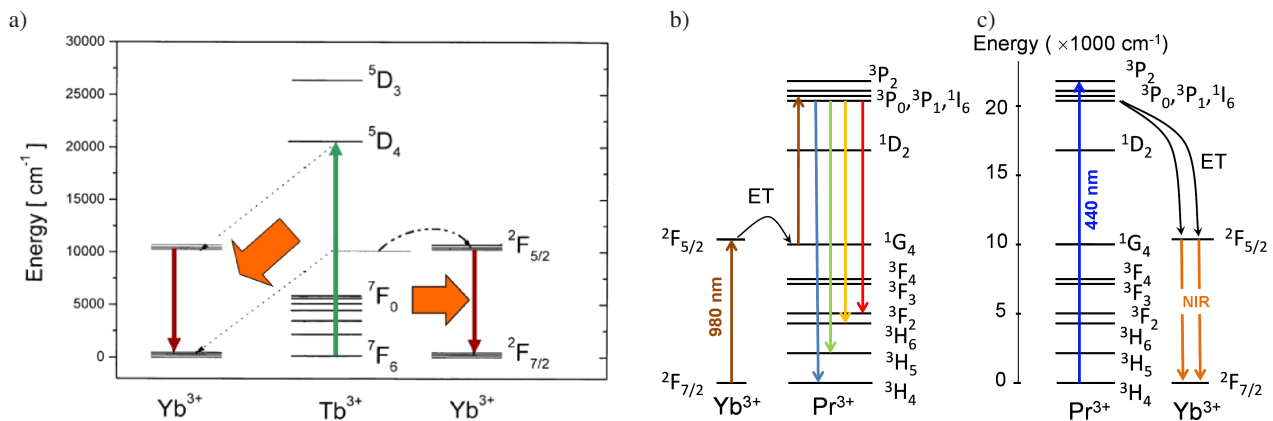


Fig. 4. a) The Tb<sup>3+</sup>: <sup>5</sup>D<sub>4</sub> energy level corresponds at about twice the energy of the Yb<sup>3+</sup>: <sup>2</sup>F<sub>5/2</sub> energy level. The Yb<sup>3+</sup> ions don't present an energy level above the <sup>2</sup>F<sub>5/2</sub> level up to the UV region. The cooperative energy transfer between a Tb<sup>3+</sup> ion and two Yb<sup>3+</sup> ions can be the main relaxation route to achieve the NIR luminescence of the Yb<sup>3+</sup>. Therefore two NIR photons are emitted by Yb<sup>3+</sup> ions after the absorption of a single photon by a Tb<sup>3+</sup> ion after Ref. 30; b), c) energy level diagram showing the possible energy transfers between Pr<sup>3+</sup> and Yb<sup>3+</sup> ions in (b) up-conversion and (c) down-conversion processes. In the up-conversion mechanism, 980 nm excitation and energy transfer Yb<sup>3+</sup> → Pr<sup>3+</sup> results in visible emission. The similar process described in Fig. 4(a) is valid even for Pr<sup>3+</sup> → Yb<sup>3+</sup> quantum cutting where a blue photon leads to two NIR photons. Here the host matrix is constituted by ZrF<sub>4</sub>-based bulk and planar waveguide glass ceramics after Ref. 31

Concerning the role of nanocrystals as rare earth sensitizers, SnO<sub>2</sub> nanocrystals constitutes a textbook example [12–14]. SnO<sub>2</sub> is a wide band-gap ( $E_g = 3.6$  eV at 300 K) n-type semiconductor and exhibits a maximum phonon energy of about 630 cm<sup>-1</sup>. The rare earth ion can be incorporated in the SnO<sub>2</sub> nanocrystal and, in the case of the Eu<sup>3+</sup> doped SiO<sub>2</sub>-SnO<sub>2</sub> system, Eu<sup>3+</sup> ions were found to substitute for the Sn<sup>4+</sup> ions in the cassiterite-structured SnO<sub>2</sub> nanocrystals [12, 13].

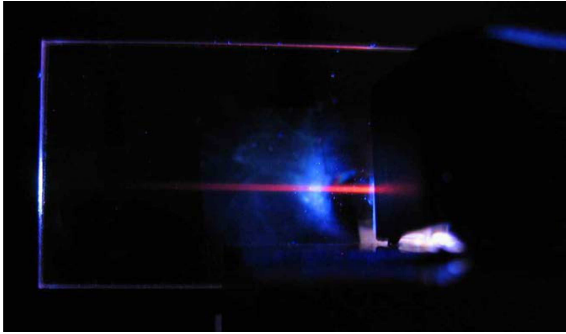


Fig. 5. Crack-free and low loss glass ceramic waveguide 75SiO<sub>2</sub>-25SnO<sub>2</sub>: Eu<sup>3+</sup> fabricated by sol-gel, dip-coating method. The photograph shows the red emission obtained pumping at 351 nm the TE<sub>0</sub> mode after Ref. 13

What is interesting in terms of energy transfer are the results regarding the luminescence enhancement observed in 75SiO<sub>2</sub>-25SnO<sub>2</sub> glass-ceramic waveguides activated by Eu<sup>3+</sup> ions. In fact, <sup>5</sup>D<sub>0</sub> → <sup>7</sup>F<sub>2</sub> excitation spectra shows that the intensity of the 320 nm SnO<sub>2</sub> absorption band increases by about 15 times, moving from 8 to 25 mol% of SnO<sub>2</sub>. This behavior reflects an increase in the number of the Eu<sup>3+</sup> ions embedded in the SnO<sub>2</sub> nanocrystals (Eu<sup>3+</sup>:SnO<sub>2</sub>) with the SnO<sub>2</sub> content and demonstrates the importance of exciton mediated energy transfer from SnO<sub>2</sub> nanocrystals to the rare earth ions.

#### 4. Rare earth-doped spherical microresonators

Microresonators are small resonators of dimensions that can range from 30 μm to 1 mm [33].

Generally they can be produced in different shape, of different materials and by different methods. The simplest microresonator is a silica microsphere which can be made by simply melting the tip of a standard telecom optical fiber by a oxy-gas torch or by an electrical spark. After the fiber melts, the surface tension will form it into a perfect sphere. This kind of silica microresonator can exhibit very high Q-factors (10<sup>7</sup> up to 10<sup>9</sup>), Q-factor defined as the average number of round trips a photon can take inside a resonator before being absorbed or scattered inside the microresonators. The light is confined by total internal reflection, so that the light is traveling along the circumference of the resonator. The modes of such resonators are called whispering gallery modes (WGM). In addition to the high quality factors the WGM also have a very low mode volume which means that we can confine light in a very small volume for a long period of time. This makes them very useful for different applications such as sensing

[34], lasers and amplifiers [35], optoelectronic oscillators or non-linear optics [36].

Such microresonator can be coated by RED films with suitable refractive index and thickness in order to tailor the WGMs luminescence [33]. The measurement of the whispering gallery modes are done using a microsphere-taper coupling setup. The coupling of light inside the sphere is achieved using a tapered fiber. The pump laser inside the microsphere is absorbed by Er<sup>3+</sup> ions inside the coating which in turn emit around 1550 nm. The emission will be greatly enhanced at wavelengths which correspond to the WGMs of the microsphere. This emitted light is then coupled out of the sphere and into the taper and detected by an optical spectrum analyzer. A typical WGM luminescence spectrum is shown in Fig. 6. The modes presented in Fig. 6 are attributed to the fundamental, or more external, whispering gallery mode since the internal modes are more difficult to couple light in and/or out of and therefore are less likely to be visible.

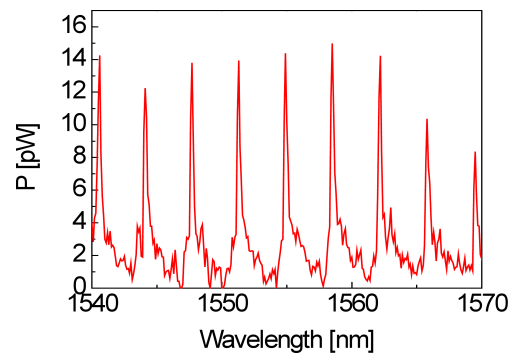


Fig. 6. The WGM luminescence of a silica microsphere of 150 μm in diameter coated by a film of composition 70SiO<sub>2</sub>-30HfO<sub>2</sub> activated with 0.3% mol Er<sup>3+</sup>

In Fig. 7 a lasing spectrum of a coated microsphere is shown. If the coating is thick enough so that the number of erbium ions interacting with the electric field of the WGMs is high enough, the stimulated emission gain can become greater than the cavity round trip loss and the sphere will start to lase. In Fig. 7 we can see the lasing spectrum of a WGM with the peak power of 280 nW.

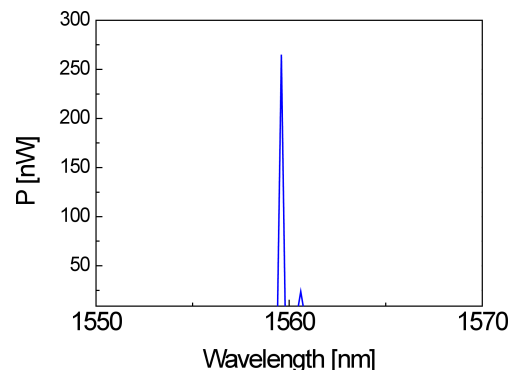


Fig. 7. Lasing action in a silica microsphere of 150 μm in diameter coated by a film of composition 70SiO<sub>2</sub>-30HfO<sub>2</sub> activated with 0.3%mol Er<sup>3+</sup>

## 5. Conclusions

Rare-earth-doped glasses play a crucial role for the development of specific photonic components, like integrated optical amplifiers, whose characteristics are critical for achieving the flat and broadband optical gain that seems needed in future communication systems. Nevertheless glass photonics is driving a huge of human activities and this fact spurs both the technical and scientific research in the field of material science and photonics.

Here we have just discussed a few examples regarding integrated optics and microcavities. We believe that the systems that have been reported here, concerning the basic properties of rare-earth-activated glasses and their application are enough to clearly demonstrate the large region of knowledge development that stay behind glass photonics. Transparent glass ceramic photonic systems have demonstrated to be crucial for several applications and especially in integrated optics. The importance of these nanocomposite materials is evident when luminescence efficiency and attenuation losses are the more important requirements. The immediate problems to solve are: (i) reproducible fabrication protocols; (ii) modelling of transparency constraints including disorder; (iii) enhance solubility for the rare earth ions.

Moving to microresonators the section presented here is far to be exhaustive of this exciting topic. In fact, their applications span from photonic engineering to quantum electrodynamics, to optical sensing and optomechanics. Even for these system fabrication protocols are crucial. Optimization of the coupling efficiency is the more important challenge for the large employment of these systems.

We can therefore conclude that the prospects of glass photonic are still very good, with continuously growing applications in the area of integrated optics, lasing, lightning, frequency converters and sensing. Optimization of the synthesis processes of glasses tailored for the specific application and of the confined structures fabrication technologies may guarantee that new record performances of RED glass based photonic devices will be achieved.

**Acknowledgements.** This research was performed within the framework of the CNR-PAS (2014–2016) joint project “Nanostructured systems in opal configuration for the development of photonic devices” and MAE Significant Bilateral Project between Italy and Egypt “Smart optical nanostructures for green photonics” (2013–2015). R.R. Gonçalves and M. Ferrari acknowledge Brazilian Scientific Mobility Program “Ciências sem Fronteiras”.

Let us to thank a number of young colleagues who are closely collaborating on this topic. Some of them are working at their PhD thesis: Simone Normani, Anna Piotrowska, Iustyna Vasilchenko, other are highly appreciated for their invaluable technical support: Cristina Armellini, Alessandro Carpentiero, Maurizio Mazzola, Stefano Varas.

## REFERENCES

[1] F. Gan and L. Xu, *Photonic Glasses*, World Scientific Publishing, London, 2006.

- [2] M. Ferrari and G.C. Righini, “Rare-earth-doped glasses for integrated optical amplifiers”, in *Physics and Chemistry of Rare-Earth Ions Doped Glasses*, Chapter 3, Trans Tech Publishers, Lausanne, 2008.
- [3] M. Ferrari and S. Taccheo, “Special section on glass photonics for integrated optics”, *Opt. Eng.* 53 (7), CD-ROM (2014).
- [4] R. Stepien, J. Cimek, D. Pysz, I. Kujawa, M. Klimczak, and R. Buczynski, “Soft glasses for photonic crystal fibers and microstructured optical components”, *Opt. Eng.* 53, 071815-1/23 (2014).
- [5] A.B. Seddon, N.S. Abdel-Moneim, L. Zhang, W.J. Pan, D. Furniss, C.J. Mellor, T. Kohoutek, J. Orava, T. Wagner, and T.M. Benson, “Mid-infrared integrated optics: versatile hot embossing of mid-infrared glasses for on-chip planar waveguides for molecular sensing”, *Opt. Eng.* 53, 071824-1/9 (2014).
- [6] D. Dorosz, J. Zmojda, and M. Kochanowicz, “Broadband near infrared emission in antimony-germanate glass co-doped with erbium and thulium ions”, *Opt. Eng.* 53, 071807-1/5 (2014).
- [7] J. Lousteau, N. Boetti, A. Chiasera, M. Ferrari, S. Abrate, G. Scarciglia, A. Venturello, and D. Milanese, “Er<sup>3+</sup> and Ce<sup>3+</sup> co-doped tellurite optical fiber for lasers and amplifiers in the near infrared wavelength region: fabrication, optical characterization and prospects”, *IEEE Photonics J.* 4, 194–204 (2012).
- [8] A. Peled, A. Chiasera, M. Nathan, M. Ferrari, and S. Ruschin, “Monolithic rare-earth doped sol-gel tapered rib waveguide laser”, *Appl. Phys. Lett.* 92, 221104-1/3 (2008).
- [9] R.R. Gonçalves, G. Carturan, L. Zampedri, M. Ferrari, M. Montagna, A. Chiasera, G.C. Righini, S. Pelli, S.J.L. Ribeiro, and Y. Messaddeq, “Sol-gel Er-doped SiO<sub>2</sub>-HfO<sub>2</sub> planar waveguides: a viable system for 1.5 μm application”, *Appl. Phys. Lett.* 81, 28–30 (2002).
- [10] G. Alombert-Goget, D. Ristic, A. Chiasera, S. Varas, M. Ferrari, G.C. Righini, B. Dieudonne, and B. Boulard, “Rare-earth doped materials enhance silicon solar cell efficiency”, *SPIE 1*, CD-ROM (2011).
- [11] M.P. Hehlen, T.R. Gosnell, and A.J. Bruce, “Spectroscopic properties of Er<sup>3+</sup> and Yb<sup>3+</sup> doped soda-lime silicate and aluminosilicate glasses”, *Phys. Rev. B* 56, 9302–9318 (1997).
- [12] S.N.B. Bhaktha, F. Beclin, M. Bouazaoui, B. Capoen, A. Chiasera, M. Ferrari, C. Kinowski, G.C. Righini, O. Robbe, and S. Turrell, “Enhanced fluorescence from Eu<sup>3+</sup> in low-loss silica glass-ceramic waveguides with high SnO<sub>2</sub> content”, *Appl. Phys. Lett.* 93, 211904-1/3 (2008).
- [13] S.N.B. Bhaktha, F. Beclin, M. Bouazaoui, B. Capoen, A. Chiasera, M. Ferrari, C. Kinowski, G.C. Righini, O. Robbe, and S. Turrell, “Enhanced fluorescence from Eu<sup>3+</sup> in low-loss silica glass-ceramic waveguides with high SnO<sub>2</sub> content”, *Appl. Phys. Lett.* 93, 211904-1/3 (2008).
- [14] S. Berneschi, S.N.B. Bhaktha, A. Chiappini, A. Chiasera, M. Ferrari, C. Kinowski, S. Turrell, C. Trono, M. Brenci, I. Cacciari, G. Nunzi Conti, S. Pelli, and G.C. Righini, “Highly photorefractive Eu<sup>3+</sup> activated sol-gel SiO<sub>2</sub> – SnO<sub>2</sub> thin film waveguides”, *Proc. SPIE*. 7604, 76040Z-1/6, (2010).
- [15] M. Mattarelli, M. Montagna, K. Vishnubathla, A. Chiasera, M. Ferrari, and G.C. Righini, “Mechanisms of silver to erbium energy transfer in silicate glasses”, *Phys. Rev. B* 75, 125102-1/6 (2007).
- [16] A. Chiasera, C. Tosello, E. Moser, M. Montagna, R. Belli, R.R. Gonçalves, G.C. Righini, S. Pelli, A. Chiappini, L. Zampedri, and M. Ferrari, “Er<sup>3+</sup>/Yb<sup>3+</sup>-activated silicitanita planar waveguides for EDPWAs fabricated by rf sputtering”, *J. Non Cryst. Solids* 322, 289–294 (2003).

- [17] A. Chiasera, C. Armellini, S.N.B. Bhaktha, A. Chiappini, Y. Jestin, M. Ferrari, E. Moser, A. Coppa, V. Foglietti, P.T. Huy, K. Tran Ngoc, G. Nunzi Conti, S. Pelli, G.C. Righini, and G. Speranza, “Er<sup>3+</sup>/Yb<sup>3+</sup> – activated silica-hafnia planar waveguides for photonics fabricated by rf-sputtering”, *J. Non-Cryst. Solids* 355, 1176–1179 (2009).
- [18] O. Péron, C. Duverger-Arfuso, Y. Jestin, B. Boulard, and M. Ferrari, “Enhanced spectroscopic properties in Er<sup>3+</sup>/Yb<sup>3+</sup>-activated fluoride glass-ceramics planar waveguides”, *Opt. Mater.* 31, 1288–1291 (2009).
- [19] M. Mattarelli, M. Montagna, L. Zampedri, M. Bouazaoui, B. Capoen, S. Turrell, M. Ferrari, and G.C. Righini, “Effect of Eu<sup>3+</sup> and Ce<sup>3+</sup> codoping on the relaxation of Er<sup>3+</sup> in silica-hafnia and tellurite glasses”, *Physica Status Solidi C* 4, 793–796 (2007).
- [20] A. Bouajaj, R.R. Gonçalves, and M. Ferrari, “Sol-gel-derived erbium-activated silica-titania and silica-hafnia planar waveguides for 1.5 μm application in C band of telecommunication”, *Spectroscopy Letters: Int. J. Rapid Communication* 47, 381–386 (2014).
- [21] B. Boulard, B. Dieudonné, Y. Gao, A. Chiasera, and M. Ferrari, “Up-conversion visible emission in rare-earth doped fluoride glass waveguides”, *Opt. Eng.* 53, 071814-1/6 (2014).
- [22] R.R. Gonçalves, G. Carturan, L. Zampedri, M. Ferrari, M. Montagna, G.C. Righini, S. Pelli, S.J.L. Ribeiro, and Y. Messaddeq, “Erbium-activated HfO<sub>2</sub>-based waveguides for photonics”, *Opt. Mater.* 25, 131–139 (2004).
- [23] G. Alombert-Goget, C. Armellini, S.N.B. Bhaktha, B. Boulard, A. Chiappini, A. Chiasera, C. Duverger-Arfuso, P. Féron, M. Ferrari, R.R. Gonçalves, Y. Jestin, L. Minati, A. Monteil, E. Moser, G. Nunzi Conti, R. Osellame, S. Pelli, A. Quandt, R. Ramponi, D. N. Rao, G.C. Righini, G. Speranza, and K.C. Vishnubhatla, “Silica-hafnia-based photonic systems”, *Mediterranean J. Electronics and Communications. A special Issue on Advanced Materials and Photonics Application* 6 (1), ISSN: 1744-2400, 8–17 (2010).
- [24] N.D. Afify, G. Dalba, C. Armellini, M. Ferrari, F. Rocca, and A. Kuzmin, “Local structure around Er<sup>3+</sup> in SiO<sub>2</sub>-HfO<sub>2</sub> glassy waveguides using EXAFS”, *Phys. Rev.* 76, 024114-1/8 (2007).
- [25] Minati L., G. Speranza, Y. Jestin, and M. Ferrari, “X-ray photoelectron spectroscopy of Er<sup>3+</sup> -activated silica-hafnia waveguides”, *J. Non-Cryst. Solids* 353, 502–505 (2007).
- [26] P.A. Tick, “Are low-loss glass-ceramic optical waveguides possible?”, *Opt. Lett.* 23, 1904–1905 (1998).
- [27] A. Edgar, G.V.M. Williams, and J. Hamelin, “Optical scattering in glass ceramics”, *Curr. Appl. Phys.* 6, 355–358 (2006).
- [28] Y. Jestin, C. Armellini, A. Chiappini, A. Chiasera, M. Ferrari, C. Goyes, M. Mattarelli, M. Montagna, E. Moser, G. Nunzi Conti, S. Pelli, G.C. Righini, and G. Speranza, “Erbium activated HfO<sub>2</sub>-based glass-ceramics waveguides for photonics”, *J. Non-Cryst. Solids* 353, 494–497 (2007).
- [29] A. Chiasera, G. Alombert-Goget, M. Ferrari, S. Berneschi, S. Pelli, B. Boulard, and C. Duverger Arfuso, “Rare earth activated glass-ceramic in planar format”, *Opt. Eng.* 50, 071105-1/10 (2011).
- [30] G. Alombert-Goget, C. Armellini, S. Berneschi, A. Chiappini, A. Chiasera, M. Ferrari, S. Guddala, E. Moser, S. Pelli, D.N. Rao, and G.C. Righini, “Tb<sup>3+</sup>/Yb<sup>3+</sup> co-activated Silica-Hafnia glass ceramic waveguides”, *Opt. Mater.* 33, 227–230 (2010).
- [31] B. Dieudonné, B. Boulard, G. Alombert-Goget, A. Chiasera, Y. Gao, S. Kodjikian, and M. Ferrari, “Up- and down-conversion in Yb<sup>3+</sup>-Pr<sup>3+</sup> co-doped fluoride glasses and glass ceramics”, *J. Non-Cryst. Solids* 377, 105–109 (2013).
- [32] G. Alombert-Goget, C. Armellini, S. Berneschi, S.N.B. Bhaktha, B. Boulard, A. Chiappini, A. Chiasera, C. Duverger-Arfuso, P. Féron, M. Ferrari, Y. Jestin, L. Minati, A. Monteil, E. Moser, G. Nunzi Conti, S. Pelli, F. Prudenzano, G.C. Righini, and G. Speranza, “Glass-based erbium activated micro-nano photonic structures”, *Proc. ICTON We. A* 5 (4), 1–4 (2009).
- [33] G.C. Righini, Y. Dumeige, P. Féron, M. Ferrari, D. Ristić, and S. Soria, “Whispering gallery mode microresonators: Fundamentals and applications”, *La Rivista del Nuovo Cimento* 34, 435–488 (2011).
- [34] S. Soria, F. Baldini, S. Berneschi, F. Cosi, A. Giannetti, G. Nunzi Conti, S. Pelli, and G. C. Righini, “High-Q polymer-coated microspheres for immunosensing applications”, *Opt. Express* 17, 14694–14699 (2009).
- [35] Z.P. Cai, H.Y. Xu, G. Stéphan, P. Féron, and M. Mortier, “Red-shift in Er: ZBLALiP whispering gallery mode laser”, *Opt. Comm.* 229, 311–315 (2004).
- [36] Y.K. Chembo and N. Yu, “On the generation of octave-spanning optical frequency combs using monolithic whispering-gallery-mode microresonators”, *Opt. Lett.* 35, 2696–2698 (2010).